6098–6108 *Nucleic Acids Research, 2017, Vol. 45, No. 10* *Published online 7 March 2017*
doi: 10.1093/nar/gkx160

Random pseuoduridylation *in vivo* reveals critical region of *Escherichia coli* 23S rRNA for ribosome assembly

Margus Leppik, Aivar Liiv and Jaanus Remme*

Institute of Molecular and Cell Biology, University of Tartu, Riia 23, 51010 Tartu, Estonia

Received November 14, 2016; Revised February 20, 2017; Editorial Decision February 23, 2017; Accepted February 27, 2017

ABSTRACT

Pseudouridine is the most common modified nucleoside in RNA, which is found in stable RNA species and in eukaryotic mRNAs. Functional analysis of pseudouridine is complicated by marginal effect of its absence. We demonstrate that excessive pseudouridines in rRNA inhibit ribosome assembly. Tenfold increase of pseudouridines in the 16S and 23S rRNA made by a chimeric pseudouridine synthase leads to accumulation of the incompletely assembled large ribosome subunits. Hyper modified 23S rRNA is found in the r-protein assembly defective particles and are selected against in the 70S and polysome fractions showing modification interference. Eighteen positions of 23S rRNA were identified where isomerization of uridines interferes with ribosome assembly. Most of the interference sites are located in the conserved core of the large subunit, in the domain 0 of 23S rRNA, around the peptide exit tunnel. A plausible reason for pseudouridine-dependent inhibition of ribosome assembly is stabilization of rRNA structure, which leads to the folding traps of rRNA and to the retardation of the ribosome assembly.

INTRODUCTION

All ribosomes have a conserved structural core as revealed by crystallographic and cryo-EM studies. The conserved core is composed mostly of rRNA, which is stabilized by universal r-proteins (1). The core includes the ribosome subunit interface as well as the functional sites for decoding and peptidyl transfer. Ribosome structure forms during assembly as a result of many structural rearrangements. The pathway of rRNA folding during ribosome assembly is a key for understanding ribosome assembly process, yet our knowledge about rRNA folding and ribosome assembly is not sufficient.

Ribosome assembly in bacteria is fast and robust. About 100 molecules are involved in bacterial ribosome biogenesis. Ribosome assembly is directed by sequential association of r-protein with rRNA and by folding of rRNA. Both events start during transcription of rRNA. Association of r-proteins with pre-ribosomal particles has been studied mostly *in vitro* using ribosome reconstitution techniques. Sequential and cooperative binding of r-proteins with rRNA is characterized by the assembly map/landscape (2–5). Chemical probing experiments show that the ordered association of r-proteins into ribosome subunit is mediated by r-protein directed rearrangement of rRNA structure (6–8). Structural rearrangements during ribosome assembly are evident by the high activation energy required during ribosome subunit reconstitution *in vitro* (9,10).

Transcribed spacer sequences of rRNA operons participate in rRNA folding and ribosome assembly by making transient interactions with the structural part of rRNA (11,12). This points to an importance of the transient structures during ribosome assembly. Several single point mutations in both 16S and 23S rRNA cause ribosome assembly defects (13,14). Such mutations are likely to affect rRNA folding pathway.

In addition to the r-proteins, other protein factors interact with rRNA and direct post-transcriptional refolding of rRNA. RNA helicases SrmB and DeaD/CsdA facilitate ribosome large subunit assembly, further emphasizing an importance of structural transitions in ribosome assembly (15–17). Recognition sites for rRNA modification enzymes form during ribosome assembly as a result of rRNA folding/refolding, which is illustrated by the assembly stage specific nature of various rRNA modifications (18). At least two rRNA methylases play an important role in ribosome assembly, RsmA (KsgA) for ribosome small subunit assembly (19) and RlmE for ribosome large subunit assembly (20). RlmE catalyzed 2'O methylation of U2552 *in vitro* promotes interactions between 23S rRNA domains (20).

The most common single nucleotide modification in all rRNA species is pseudouridine (http://www.ecosal.org) (21). Until recently pseudouridine was found at conserved positions of stable RNA species such as tRNA, rRNA, snRNA. In 2014 pseudouridines were found in numerous eukaryotic mRNA species (22–24).

*To whom correspondence should be addressed. Tel: +372 7 375 031; Email: jremme@ut.ee

Escherichia coli rRNA contains 11 pseudouridine residues, 1 in 16S rRNA and 10 in 23S rRNA (21). For comparison, yeast *Saccharomyces cerevisiae* ribosome contains 44 pseudouridines (25). In bacteria pseudouridines are made by specific enzymes. Seven pseudouridine synthases isomerize 11 uridines in *E. coli* rRNA. Deletion of rRNA-specific pseudouridine synthase genes in bacteria has little effect on the ribosome biogenesis or ribosome functioning (21). An exception is RluD, which isomerizes three urindines in the functionally important helix 69 (U1911, U1915, U1917). Deletion of RluD gene can cause defects in translation termination and ribosome assembly (26–28). However, this effect is observed only in a certain genetic context and can be reverted by mutations in the *prfB* (RF-2) or *prfC* (RF3) (29,30).

The second pseudouridine synthase in *E. coli* that can isomerize three uridines is RluC. RluC isomerizes U955, U2504 and U2580 of 23S rRNA (26,31). Both RluC and RluD belong to the RluA family of pseudouridine synthases. They consist of two domains: an N-terminal S4-like domain and a C-terminal catalytic domain, which are connected by a flexible linker region containing three glutamic acid residues. The N-terminal S4-like domain (residues 1–72) of RluD was proposed to be required for initial docking of the enzyme to its substrate and to be the main element for substrate specificity of the synthase (32). High flexibility of the S4-like domain is speculated to allow specific binding to the correct molecular target without producing very high affinity, avoiding the enzyme becoming trapped in unproductive enzyme–product complexes (33). The catalytic domain of the RluD involves residues 76–326 and is thought to have only minor contribution to the specificity (32). RluC modifies the 23S rRNA at early and RluD at late stage of ribosome assembly (18). Exchange of the S4 domain of pseudouridine synthase should cause major difference in substrate specificity if the S4 domain is the main determinant of specificity.

In this study, we engineered chimeric pseudouridine synthase (RluCD) containing N-terminal S4 domain of the RluC and C-terminal catalytic domain of the RluD that is able to introduce excessive pseudouridines into rRNA at nonnative positions. The chimeric enzyme (RluCD) was used as a tool to study an effect of over-modification of rRNA on the ribosome biogenesis. Excessive pseudouridylation of 23S rRNA slows down progression of ribosome assembly during early or middle stages. Modification interference approach identified the sites in 23S rRNA whose modification prevents ribosome assembly. It is plausible that pseudouridines can cause RNA misfolding when present at non-native positions.

MATERIALS AND METHODS

Plasmids and strains

Chimeric pseudouridine synthase was expressed in *E. coli* M15 strain or in CD204 strain. Both strains contain pREP4 plasmid, constitutively expressing *lac* repressor allowing repression of transcription of chimeric pseudouridine synthase RluCD.

Strain rluD114 where *yfiI* (RluD) gene had been disrupted with Km cassette (34) was used as a parent strain to construct strain CD204. The antibiotic resistivity cassette was eliminated from the rluD114 using plasmid PCP20 containing *Flp* recombinase gene (35). P1 transduction was used to transfer *yceC* (RluC) gene, disrupted with Km cassette, from JW1072 strain (36) into rluD114 strain. Double knockout was verified with polymerase chain reaction (PCR). Also high-performance-liquid-chromatography (HPLC) analysis and CMCT-alkali treatment/primer extension method (37) was used to confirm lack of the RluC and RluD pseudouridine synthases-specific pseudouridines from 23S rRNA, of the new MG1655 rluC, rluD double knockout strain (CD204). It should be noted that the strain CD204 contains a mutation D131Y in the *prfB* gene encoding RF-2. The mutation D131Y has been shown to compensate ribosome assembly defect caused by the RluD deletion (29).

Constructing chimeric pseudouridine synthase

To construct chimeric RluCD pseudouridine synthase, S4-like domain of the RluC and catalytic domain of the RluD was fused together using the identical linker region of the native proteins containing three glutamic acids. PCR primers 5′- ACC ATG GCG AAA ACA GAG ACT CCA TCC GTA AAA ATT -3′ and 5′- GCC ATG GAA CGT CTC GAA GAA GAG GCG CGT TTT GAA CCG CAG G- 3′ were used to introduce Esp3I restriction site into the DNA fragment of the RluC S4-like domain and RluD catalytic domains respectively to fuse the DNA fragments together via the linker coding sequence. PCR primers 5′- ACC ATG GCG AAA ACA GAG ACT CCA TCC GTA AAA ATT -3′ and 5′ - GCA GAT CTT AAC CAG TCC ACT TCA TCC T – 3′ were used to introduce NcoI restriction site into 5′ end and BglII restriction site into 3′ end of the RluCD gene for cloning. The RluCD was cloned between NcoI and BglII restriction sites of expression vectors pQE-60 and pBADMycHisC containing C-terminal His-6 tag.

Cell growth determination

Fresh overnight culture of M15 or CD204 strain containing plasmid with RluCD gene was diluted 20 times with 2YT medium (without antibiotics) and half of the culture was induced with IPTG (final concentration 1 mM). The cultures were grown at 37°C. A_{600} measurement was carried out from 150 μl of the culture on 96 well plate. Fresh overnight culture was also streaked out onto LB plates with or without presence of 1 mM IPTG. The LB plates were incubated overnight at 37°C.

Preparation of ribosomes and rRNA

Cells were grown at 37°C in 2xYT medium supplemented with ampicillin (100 μg/ml) and kanamycin (25 μg/ml). Ribosomes were isolated from cells 2 h after induction with IPTG (1 mM) or 6 h after induction with arabinose until attenuance of 0.3–0.4 at A_{600} was reached. Cells were collected with low-speed centrifugation, resuspended in lysis buffer and lysed by freeze-thawing as described previously (38) or resuspenden in LLP buffer (10 mM Tris/HCl (pH 8.0), 60 mM KCl, 60 mM,NH_4Cl, 12 mM MgOAc, 6 mM

2-mercaptoethanol) and lysed with Precellys24 Lysis and Homogenization (Bertin Technologies) according to manufactures protocol. Up to 100 ODU of the lysate was layered onto a 15–30% (w/w) sucrose gradient in buffer LLP and centrifuged in Beckman ultracentrifuge SW28 rotor 22 000 rpm for 16 h ($\omega^2t = 3.1 \times 10^{11}$) at 4°C. Sucrose density gradients were analyzed with continuously monitoring at 254 nm. Fractions containing ribosomal particles were collected, diluted with LLP and particles were pelleted with ultracentrifugation in 45Ti rotor 41 000 rpm for 15 h ($\omega^2t = 1.0 \times 10^{12}$). 50S and 30S pellets were dissolved in LLP and stored at −80°C. 70S pellet was dissolved in dissociation buffer (10 mM Tris/HCl (pH 8.0), 60 mM KCl, 60 mM, NH_4Cl, 1 mM MgOAc, 6 mM b-mercaptoethanol) and layered onto 15–30% (w/w) sucrose gradient in dissociation buffer and centrifuged in SW28 rotor 22 000 rpm for 18 h ($\omega^2t = 3.5 \times 10^{11}$) at 4°C. Gradients were monitored and ribosomal particles were collected as described above. Phenol–chloroform treatment and ethanol precipitation was used for rRNA extraction from ribosomal particles.

Analysis of rRNA

High-performance liquid chromatography was done according to Gehrke and Kuo (39) as described in Siibak and Remme (18). 5′-end sequencing of the 23S rRNA was carried out by primer extension using primer 23S 5′ END (5′-TCG CCT CTG ACT GCC AGG GCA TCC-3′). Avian myeloblastosis virus (AMV) reverse transcriptase (Seikagaku) was used in presence of [α-^{32}P]dCTP (Hartmann Analytic). The resulting DNA fragments were resolved in 7% polyacrylamide-urea gel. Radioactivity in polyacrylamide gel electrophoresis was visualized by Typhoon phosphor imager (GE Healthcare).

Primer extension analysis of CMCT/alkali modified RNA was performed according to (34,40). List of primers used for 23S and 5S rRNA analysis are in the Supplementary Table S1.

Time course of ribosome assembly *in vivo*

CD204 cells containing plasmid with chimeric pseudouridine synthase *rluCD* gene (CD204/pRluCD), were grown at 37°C in 180 ml of labeling medium (tryptone 10 g/l, yeast extract 1 g/l, NaCl 10 g/l), CD204 strain without the plasmid served as a control. IPTG final concentration 1 mM was added when culture A_{600} reached 0.15. Then 15 μCi of [^{3}H]-uridine (Hartmann Analytic) was added after A_{600} reached 0.3 for RNA labeling and RNA synthesis was blocked by adding 90 mg of rifampin to the culture after 5 min of incubation. Cells were collected from 50 ml of the culture with low-speed centrifugation after 0, 10 and 60 min of incubation. Collected cells were resuspended in 500 μl of LLP buffer and lysed with Precellys24 Lysis and Homogenization (Bertin Technologies) according to manufactures protocol. Lysate was layered onto 10–25% (w/w) sucrose gradient and centrifuged in SW28 rotor 20 000 rpm for 17 h ($\omega^2t = 2.7 \times 10^{11}$). Gradients were analyzed with continuously monitoring at 254 nm and fractionated into 40 fractions. High molecular-weight material was precipitated from the gradient fractions with an equal volume of 20% trichloroacetic acid (TCA). The precipitates were collected on glass fiber filters, and the incorporated radioactivity was measured by scintillation counting.

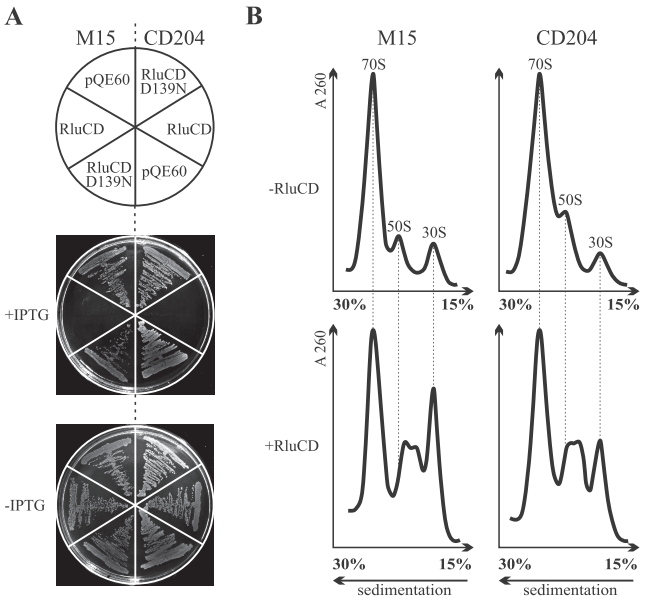

Figure 1. Expression of the chimeric pseudouridine synthase RluCD inhibits bacterial growth and ribosome assembly. (**A**) Growth assay of *wt* M15 strain and strain lacking RluC and RluD (CD204) with expression of chimeric pseudouridine synthase RluCD induced (+IPTG) or not induced (−IPTG) on LB plates. Cells transformed with catalytically inactive RluCD (RluCD D139N) and empty vector (pQE60) were used as a controls. (**B**) Sucrose gradient profiles of ribosomes of M15 and CD204 strains. M15 or CD204 cells grown without expression of chimeric RluCD pseudouridine synthase represent normal ribosomal profile in sucrose density gradient (upper panels). Dotted lines indicate the location of normal ribosomal particles in sucrose density gradients.

RESULTS

Expression of chimeric pseudouridine synthase RluCD interferes with ribosome formation

A chimeric pseudouridine synthase consisting of the N-terminal S4-like domain of RluC and the C-terminal catalytic domain of RluD (referred to as RluCD) was constructed. The chimeric protein was expressed under the control of inducible phage *T5* promoter in the *E. coli* wild-type strain M15 and in the CD204 strain lacking genes for RluC and RluD. Bacteria of both strains are not able to grow in the presence of the inducer on the agar plates (Figure 1A) and causes highly prolonged lag phase in liquid medium (Supplementary Figure S1). Induction of the RluCD at the exponential growth phase leads to severe inhibition of translation while transcription is only slightly affected (Supplementary Figure S2). Next experiments were set up to define the step in translation that is affected by chimeric pseudouridine synthase.

Ribosomal particle composition of both M15 and CD204 strains was analyzed 2 h after induction of the RluCD using sucrose gradient centrifugation. In both strains, the expression of chimeric enzyme leads to the loss

of 50S peak and accumulation of two types of unusual particles sedimenting between the 30S and 50S ribosome subunits (Figure 1B). These unusual particles are tentatively assigned as 42S and 48S particles (Supplementary Figure S3). Accumulation of such particles suggests that the ribosome large subunit assembly is affected in the presence of RluCD. It must be noted that the strain CD204 contains a mutant form of RF-2 (D131Y) that suppresses ribosome assembly defect caused by the deletion of the RluD (29). Expression of the chimeric RluCD caused effect on the ribosome assembly in the strains CD204 strain and *wt* M15 strain is nearly identical (Figure 1).

For comparison, the effect of the expression of RluCD under the arabinose inducible *araBAD* promoter on bacterial growth and ribosome assembly was tested. Expression of the RluCD in this system inhibited bacterial growth as it was observed with *T5* promoter, albeit a longer time of RluCD expression was needed to achieve a similar extent of ribosome assembly defect. Expression of RluCD under the control of *araBAD* promoter led to accumulation of similar subribosomal particles as was observed with the *T5* promoter (Supplementary Figure S4A).

A possibility that expression of RluCD protein itself inhibits ribosome assembly by binding to the precursor particles and blocking the assembly of r-proteins was tested by expression of catalytically inactive variant of the RluCD where catalytic Asp139 (RluD numbering)was replaced with Asn (41). Expression of the catalytically inactive RluCD in CD204 strain does not affect the cell growth (Figure 1A and Supplementary Figure S1), nor ribosome assembly according to the sucrose gradient profile (Supplementary Figure S5), indicating that the phenotypic effects are caused by the catalytic activity of the chimeric pseudouridine synthase RluCD.

Subribosomal particles have an incomplete protein composition

Ribosomal proteins bind to the rRNA in an ordered way which is characterized by ribosomal protein assembly maps of the small and large subunits (2,3). Fully assembled ribosomes contain a complete set of r-proteins, one copy each (42). Therefore, the r-protein composition is an important indicator of the stage of ribosome assembly. Ribosomal protein content was determined by qMS using SILAC labeling. 30S, 42S, and 48S ribosomal particles were isolated from the strain CD204/pRluCD (as shown in Supplementary Figure S3) and their protein composition was determined using *wt* 70S ribosomes with labeled Arg and Lys as standards (Figure 2). Free 30S particles contain most SSU proteins, same amount as in the standard 70S ribosomes (Figure 2A). Only the proteins S1, S2 and S21 are present in slightly reduced level in SSU (Figure 2A). These proteins are weakly associated with the SSU and are among the last proteins bound during ribosome assembly *in vivo* (43). Thus, majority of the free 30S particles are completely assembled or are in the late assembly stage. In contrast, ribosomal particles of the 42S fraction contain only 10 LSU proteins over 80%. Among them early assembly essential proteins L3, L13, L20 and L24 (Figure 2B). Proteins L16, L27, L28, L33, L35 and L36 present at 30% or less in the 42S particles (Figure 2B)

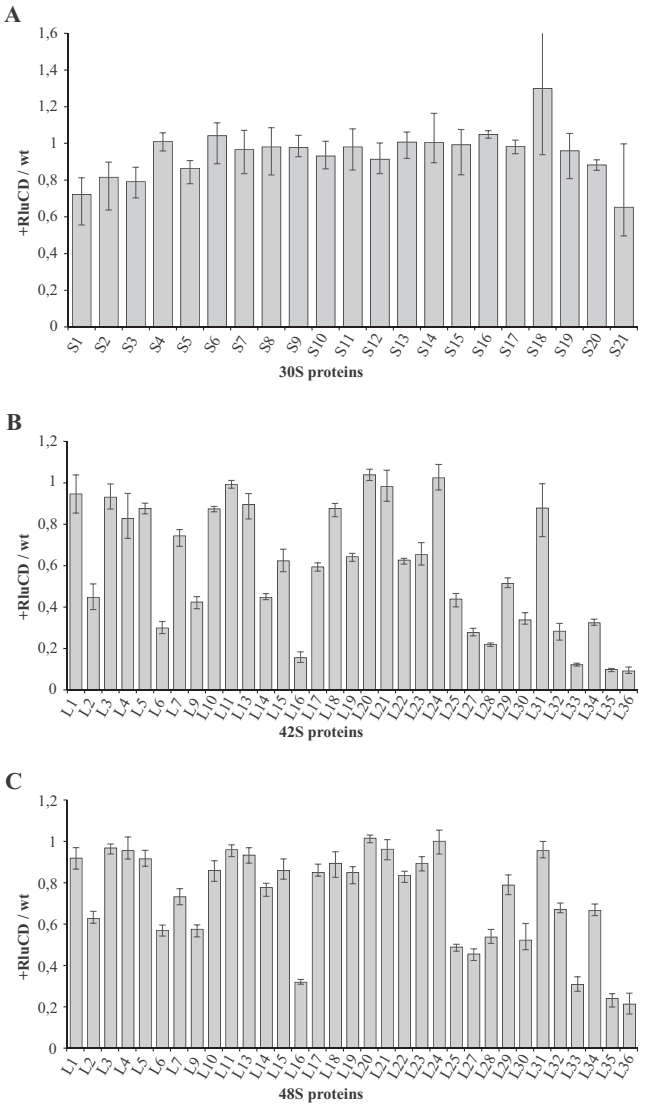

Figure 2. LSU related subribosomal particles but not SSU related particles contain substochiometric amounts of r-proteins. Ribosomal particles of the *Escherichia coli* CD204 were isolated after expression of RluCD for 2 h. Subribosomal particles were mixed with stoichiometric amount of standard 70S ribosomes containing 'heavy' proteins. Proteins were digested with trypsin or LysC and the 'light'/'heavy' ratio of peptides was determined by HPLC-MS/MS. (**A**) Amount of s-proteins in 30S particles; (**B**) Amount of L-proteins in 42S particles; (**C**) Amount of L-proteins in 48S particles. Error bars represent SD of two independent experiments.

belong to the late assembly proteins (10). 48S particles contain most LSU proteins at stoichiometric level (Figure 2C). However, several late assembly LSU proteins (L16, L25, L27, L33, L35 and L36) are found with less than 50% of the functional subunit level (Figure 2C). Notably, protein L16 is required for the late assembly events (3). Thus, 42S particles resemble ribosome early assembly intermediate and 48S particles have similar protein composition to the late assembly intermediates. The protein composition of the LSU related particles indicates that catalytic activity of the RluCD causes misassembly of the ribosomal large subunit.

RluCD isomerizes many uridines of rRNA in a non-specific manner

Pseudouridine content in the ribosomal particles was quantified by reverse-phase HPLC (39) (Figure 3), the method that allows quantitative analysis of nucleosides (44). Synthesis of RluCD was induced for 2 h in the M15 and CD204 strains and the ribosomal particles were separated by sucrose gradient centrifugation (shown in Supplementary Figure S3). 70S ribosomes were dissociated into 30S and 50S subunits (referred to as D30S and D50S where D stands for dissociated). Nucleosides were prepared and separated by reverse-phase HPLC. A remarkable increase in pseudouridine content of the rRNA is evident (Figure 3B and C). 16S rRNA of the free 30S fraction contains 12–14 pseudouridine residues instead of the expected single natural pseudouridine, i.e. over 10 additional unspecific pseudouridines were found (Figure 3B). 30S protein composition and subunit sedimentation as single 30S peak show that the extra pseudouridine residues in 16S rRNA do not cause major assembly defects of the 30S subunit. Therefore, we concentrated further analysis on the ribosome large subunit. In the rRNA of 42S particles over 60 pseudouridines per 23S rRNA are found, which equates with over 50 additional unspecific pseudouridines (Figure 3C). In the 48S particles, 30–35 additional pseudouridine residues were found. In comparison, the 16S and 23S rRNA isolated from the 70S ribosomes contain only 5–7 additional pseudouridine residues (Figure 3B and C). The total number of extra pseudouridines does not significantly depend upon presence of chromosomal RluC and RluD as the same number of extra pseudouridine per 23S rRNA is present in the double deletion strain CD204 and in the *wt* strain (Figure 3B and C). The fact that 16S and 23S rRNAs in 70S ribosomes contain significantly less pseudouridine residues as compared to the subribosomal particles suggests that the excessive pseudouridines in rRNA species cause strong selection against 70S ribosome pool.

Psudouridine content of rRNA in the polysomes was determined. Polysomes were isolated by sucrose gradient centrifugation 2 h after induction of RluCD (Supplementary Figure S6A). Nucleoside composition of 16S and 23S rRNA was determined as above after dissociation of ribosome subunits. Polysomal 16S rRNA contain 6 and 23S rRNA 5 additional pseudouridines (Supplementary Figure S6B). Thus, rRNA in the polysomes contain similar fraction of RluCD dependent pseudouridines as it was observed in the 70S ribosomes. This observation suggests that RluCD dependent isomerization of uridines at low level does not inactivate ribosomes.

Similar effects on the ribosome assembly were also observed when the alternative expression system of RluCD under the control of arabinose inducible *araBAD* promoter was used (Supplementary Figure S4A). Nucleoside analysis by HPLC demonstrates that this system yields significantly higher amounts of pseudouridines in the rRNA. 23S rRNA in the 42S, 48S and 70S ribosomes contained 82, 66 and 42 pseudouridines, respectively (Supplementary Figure S4B).

A possibility that chimeric pseudouridine synthase RluCD isomerizes unspecific uridines in tRNA was tested. In this respect, nucleoside analysis was performed on tRNA from *E.coli* cells expressing RluCD. We did not find any difference in number pseudouridines in tRNA purified from RluCD induced and uninduced cells (Supplementary Figure S6C). This result clearly demonstrates that tRNA is not a substrate for RluCD and modification of tRNA is not the cause of phenotypic effects seen in this work.

In contrast, the HPLC analysis demonstrated that 23S rRNA modifications m^5C, m^5U and Um are present at low level in the 42S and 48S particles (Supplementary Figure S7). Formation of Um is known to occur during late stages of ribosome large subunit assembly (18,45,46) while m^5C and m^5U are formed during intermediate stages of LSU assembly (18). Thus, the reduced level of assembly-dependent modifications in the 42S and 48S particles confirms that expression of RluCD induces defects in the ribosome large subunit assembly. These results suggest that isomerization of uridines to pseudouridines at non-native positions hinders large ribosome subunit assembly.

It is known that rRNA 3′ and 5′ end trimming occur after the assembly of the ribosome subunit is complete (47). Thus, the length of rRNA 3′ and 5′ ends are important determinates of ribosome assembly state. Mapping of the 5′ ends of 23S rRNA further confirms the assembly deficiency of the 42S and 48S particles. In the subribosomal particles, the 23S rRNA is incompletely processed while the 70S ribosomes contain a mature 5′ end (Supplementary Figure S8). Processing of 23S rRNA is known to occur during last steps of ribosome assembly at the level of translating ribosomes (48).

Functional activity of both ribosome subunits derived of 70S and polysome fraction was compared with the wild-type subunits using fMet-Puromycin assay. 30S and 50S subunits were incubated with f[^{35}S]Met-tRNA followed by short incubation with puromycin. Formation of f[^{35}S]Met-puromycin is a measure of functional 70S. 30S subunits of 70S and polysome fraction of RluCD expression strain were compared to the *wt* 30S subunits in 50S titration assay. 50S subunits of RluCD expressing strain exhibited similar activity as compared to the 50S standard isolated from *wt* strain (Supplementary Figure S9). Moreover, functional activity of 30S subunits derived of 70S or polysomes of RluCD expression strain was apparently equal to the *wt* 30S. Thus, expression of RluCD does not interfere with the functional activity of assembled ribosomes that are able to reach to the functional 70S pool both according to pseudouridine content in polysomes and peptide bond formation assay.

Expression of RluCD reduces the rate of ribosome subunit assembly

Time course of ribosome subunit formation was determined in the strain CD204 using RNA pulse labeling with and without induction of RluCD synthesis. RNA was labeled with [^{3}H]uridine during 5 min and transcription initiation was stopped by adding rifampicin at time point 0. Cells were collected at different time points and incorporation of rRNA into ribosomes was determined from sucrose gradient centrifugation. Ribosome profiles at time points 0, 10 and 60 min after stopping transcription initiation are shown in Figure 4. At the 0 time point of the uninduced control cells the radioactive RNA is found in the 70S, 50S, 30S and

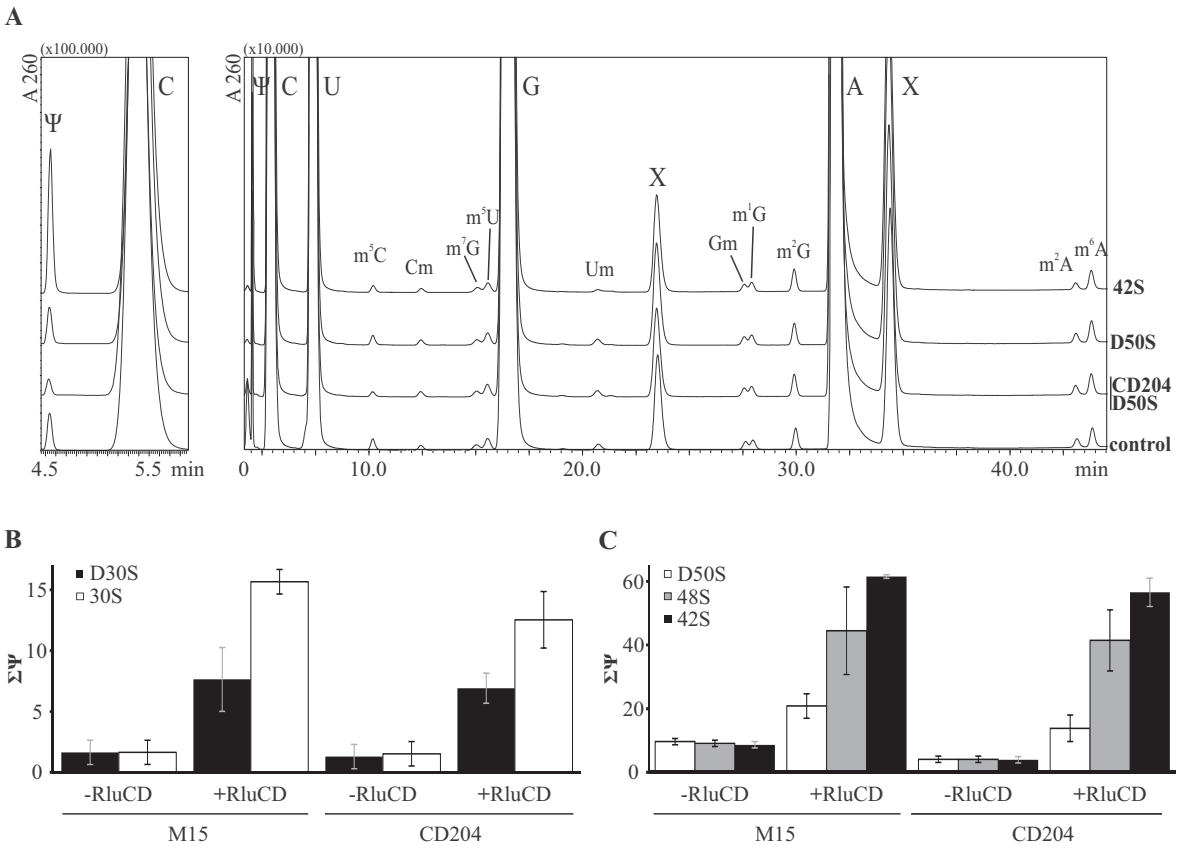

Figure 3. Chimeric pseudouridine synthase RluCD isomerizes excessive uridines in both 16S and 23S rRNA *in vivo*. (**A**) HPLC chromatogram of 23S rRNA nucleosides isolated from *Escherichia coli* CD204/pRluCD. 23S rRNA was isolated from 42S, 48S particles and 50S particles dissociated from 70S ribosomes (D50S) of cells where expression of RluCD was induced for 2 h. Control 23S rRNA was isolated from mature 50S subunits of of *wt* strain. Left panel of the chromatogram represents zoom in of pseudouridine peak. Peaks corresponding to rRNA modifications are indicated and X corresponds to unknown compounds. (**B**) Number of pseudouridine residues per 23S rRNA in the LSU-related particles of M15 and CD204 the RluCD was induced and uninduced. (**C**) Number of pseudouridine residues per 16S rRNA in the SSU-related particles of M15 and CD204 the RluCD was induced and uninduced. Number of pseudouridines was calculated from HPLC chromatogram peak areas corresponding to pseudouridine. Error bars represent SD of two independent experiments.

top fractions (Figure 4A). About 10 min later, the majority of the [^{3}H] label has moved into the 70S fraction (Figure 4A) in agreement with the known rate of ribosome assembly in the *wt* strain (17,49). In contrast, expression of RluCD leads to a severe ribosome assembly defect as evident from accumulation of [^{3}H]uridine containing RNA preferentially in the top fraction of the sucrose density gradient (Figure 4B). A small amount of rRNA is incorporated into ribosomal fractions but with a delay compared to the *wt* strain, showing that progression of the ribosome subunit assembly is retarded (note the different scales in Figure 4A and B). Even after 1 h only a small amount of radioactivity was present in the 70S fraction (Figure 4B). It has to be noted that same amount of radioactively labeled [^{3}H]uridine was used in the experiments and the low level of radioactivity counted in the ribosome fractions of sucrose density gradients (Figure 4A and B) can be explained with turnover of rRNA. Ribosome assembly defect causes degradation of unassembled rRNA and accumulation of small RNA fragments on the top of gradient. Very small RNA fragments and nucleotides do not precipitate with TCA. Thus, the rate of ribosome assembly is drastically reduced. Moreover, 42S and 48S particles can reflect accumulation of early and late assembly intermediate particles. Thus, expression of the chimeric enzyme RluCD blocks ribosome assembly at intermediate and late stages. One possible reason for ribosome assembly inhibition by excessive pseudouridines is stabilization of folding intermediates i.e. reducing the rate of rRNA refolding during large subunit assembly.

Identification of the positions of pseudouridines interfering ribosome assembly

Positions of pseudouridylation were identified on entire 23S rRNA from 42S, 48S and 70S ribosomal particles of both *T5* promoter and *araBAD* promoter driven expression of RluCD in the strain CD204 (Supplementary Table S1). Primer extension stop sites specific to the CMCT/alkali modified lanes correspond to the pseudouridines (Figure 5). Pseudouridines were identified at native positions, which can be attributed to the RluA, RluE, RluB and RluF and at 229 (of total 591 U in 23S rRNA) non-native positions. Non-native pseudouridine residues are nearly uniformly distributed along the 23S rRNA sequence in both expression systems (Figures 5 and 6A). A few unmodified islands

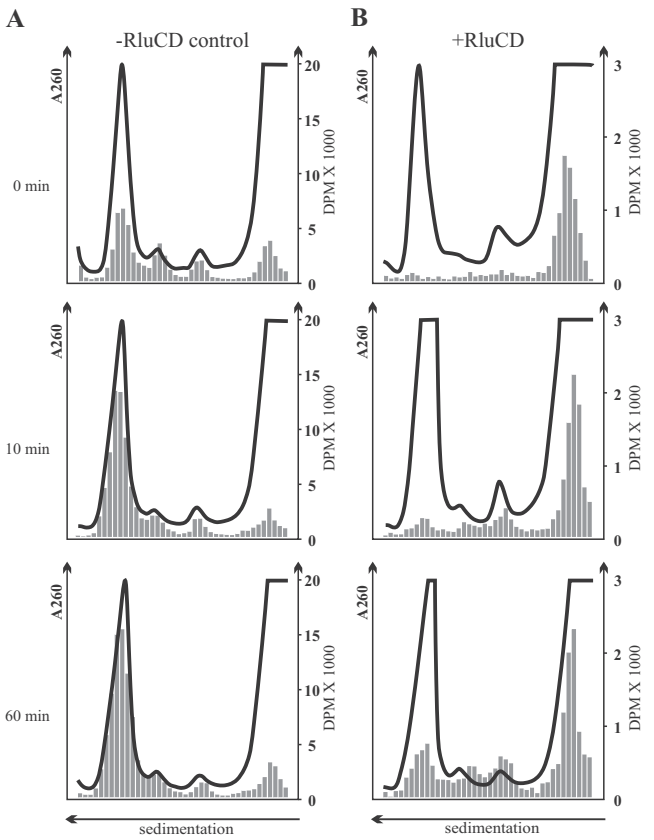

Figure 4. Chimeric pseudouridine enzyme RluCD impedes ribosome assembly. *Escherichia coli* CD204/pRluCD cells were grown until early exponential phase, and [^{3}H]uridine was added to the culture for RNA labeling. Transcription was stopped after 5 min of labeling by rifampicin. Culture aliquots were taken at different time points (0, 10 and 60 min; 0 min indicates the addition of rifampicin). Cells were lysed and ribosomal particles were separated in sucrose density gradients. Sucrose gradients were fractionated ribosomal particles were precipitated with TCA and analyzed for radioactivity to determine the time course of ribosome assembly. Optical profile of sucrose density gradient is shown by solid line and TCA precipitated [^{3}H]uridine is shown as gray columns. (**A**) Time course of the ribosome assembly without induction of RluCD. (**B**) Time course of the ribosome assembly with induction of RluCD. Note the different scales in panels A and B.

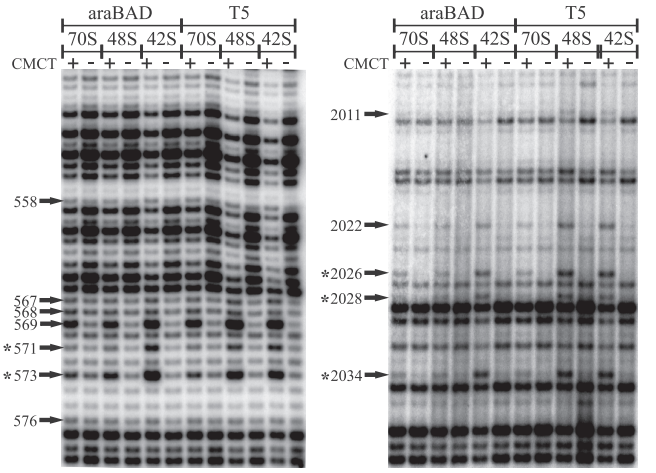

Figure 5. Identification of pseudouridylation interference sites in 23S rRNA. Ribosomal particles were isolated form cells after expression of the chimeric enzyme RluCD for 2 h. RNA was isolated from ribosomal particles and positions of pseudouridines were identified by CMCT/alkali treatment using reverse transcriptase directed primer extension. Pseudouridines are at positions where CMCT specific band is present in +CMCT line and is absent in −CMCT line. Numbers and arrows indicate the positions of pseudouridines in 23S rRNA, asterisks mark position where pseudouridylation interference was found.

appear on the secondary structure map, e.g. helices 42–44, 86–88 and 95 (Figure 6A). RluCD directed isomerization of uridines does not apparently depend on any primary sequence elements. Base-paired and single-stranded uridines are isomerized nearly at equal level (Figure 6A). In general the pseudouridylation pattern of 23S rRNA of the 70S, 48S and 42S particles is similar. However, isomerization of uridines at 18 positions was readily detected in the 42S and 48S particles but significantly less or none in the 70S ribosomes (examples are shown with asterisks in Figure 5). Notably, only small quantitative differences of pseudouridylation level can be found between 42S and 48S particles. The region 567–576 is rich of uridines. U567 and U568 are isomerized at low, U569 at high level but all three are present equally in 42S, 48S and 70S particles. In contrast, pseudouridine at 571 and 573 is found in the 42S and 48S but significantly less in 70S ribosomes (Figure 5). The positions which are isomerized preferentially in subribosomal particles (42S and 48S) are referred to as 'interference sites' (499, 571, 573, 1130, 1132, 1258, 1267, 1273, 1856, 1880, 1886, 1940, 1944, 2026, 2028, 2034, 2111 and 2324) (labeled red on Figure 6A and B). One interference site was found in the domain I (U499), two sites in the domain II (U1130, U1132), none in the domain III, five sites in the domain IV (1856, 1880, 1886, 1940 and 1944), two in the domain V (2111 and 2324), none in the domain VI and eight in the recently defined domain 0 (571, 573, 1258, 1267, 1273, 2026, 2028 and 2034). The domain 0 is highly conserved structural element, which is anchoring other domains (50) (Figure 6A). Interference sites are located in the central part of the domain 0 (helices 25a, 26, 26a and 72). Notably, three pairs of interfering pseudouridines are juxtaposed for base-pairing on the opposite sides of helix 68 (1856 and 1886), bulge loop of helix 71 (1940 and 1944), and helix 72 (2028 and 2034). Fifteen interference sites are clustered on the secondary structure and three (499, 2111 and 2324) are located at distinct sites.

Clustering of interfering pseudouridines is even more evident on the level of the ribosome tertiary structure (Figure 6B). While native pseudouridines are surrounding entry of the nascent peptide tunnel (Figure 6B blue spheres), 10 out of 18 interference sites are surrounding central and distal regions of the tunnel and two are close to the tunnel entry (Figure 6B red spheres). Interference sites outside of the tunnel region are located near the L1 binding region (2111), in the cleft between L1 stalk and central protuberance (1856, 1880 and 1886), and one interference site is in the central protuberance (2324). Importantly, none of the known 23S rRNA type molecules has pseudouridine in any of the interference sites (51).

Taken together, the results of the modification interference strongly suggest that modification of specific uridines

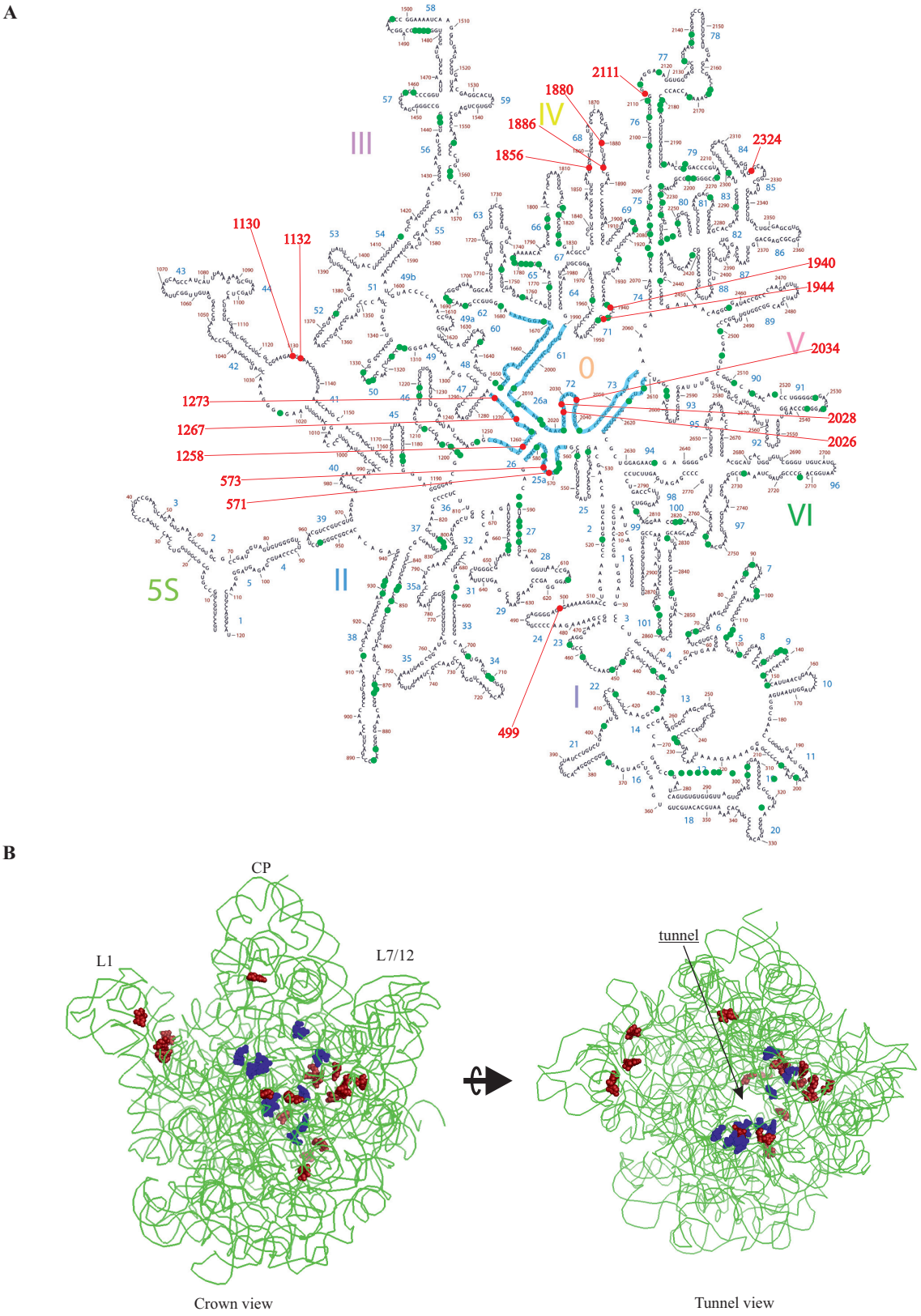

Figure 6. Distribution of RluCD dependent pseudouridines in 23S rRNA secondary and tertiary structures. (**A**) Pseudouridines identified in 23S rRNA mapped into 23S rRNA secondary structure. 23S rRNA positions where pseudouridines are distributed equally in all ribosome particles (42S, 48S and 70S) are colored green and interfering pseudouridine positions selected against 70S fraction are colored red and indicated by numbers. Recently defined 23S rRNA central domain (Domain 0) is colored cyan. (**B**) Location of modification interference sites in the 23S rRNA tertiary structure. 50S subunit (coordinates from PDB ID: 3R8S) 'crown' view and 'tunnel entry' view. Blue—native pseudouridine positions; red—interfering pseudouridine positions.

of 23S rRNA is the main reason for hindering ribosome assembly by expression of RluCD.

DISCUSSION

Ribosome assembly and structure is robust, rRNA can tolerate very many single point mutations without loss of functionality (13,14). Only a few single point mutations were found to affect ribosome large subunit assembly (14). In contrast, addition of extra pseudouridines to the ribosome appears to primarily affect ribosome assembly. Modification interference experiments together with ribosome assembly analysis demonstrate that pseudouridines at specific positions of 23S rRNA drastically reduce the rate of ribosome assembly. Distribution of interfering positions shows that inhibition of ribosome assembly is restricted to isomerization of uridines at certain 23S rRNA regions. Interfering pseudouridines are clustered both on the level of secondary and tertiary structure. Majority of the interfering positions are in the single-stranded regions in the vicinity of tertiary interaction sites.

Pseudouridines have been shown to stabilize RNA structure (52). Pseudouridine base pairs with any of the four major bases are more stable than their U equivalents (53,54). Three pseudouridine residues in the H69 stabilize both base-pairing and base stacking in this functionally important structural element (55). High-resolution crystal structure of the *E. coli* ribosome demonstrates that six of the seven well-ordered pseudouridines are involved in water-mediated contacts between the pseudouridine N1 imino groups in the major groove and the rRNA phosphate backbone, which can explain the stabilizing effect of pseudouridine (56). On the other hand, rRNA is known to undergo significant conformational changes during ribosome assembly (8,43,57). During stepwise conformational changes, new binding sites for r-proteins and recognition sites for rRNA modification enzymes are created. Importance of the rRNA structural re-organization during ribosome assembly is also emphasized by the large activation energy during ribosome reconstitution and by involvement of RNA helicases during ribosome assembly *in vivo* (9,17). Taken together, pseudouridines can stabilize rRNA structure and thereby inhibit rRNA structural transitions, which leads to the folding traps of rRNA and to the retardation of the ribosome assembly. Only early assembly proteins whose binding does not need significant conformational changes in rRNA are found at high level in the subribosomal particles. Pseudouridylation directed conformational rigidity inhibits assembly of late assembly specific proteins whose binding needs rRNA structural rearrangements.

Inhibition of rRNA refolding by pseudouridines is supported also by the fact that interfering positions are located inside the ribosome. Thus, uridines at these positions are available for isomerization only during a short time window during ribosome assembly. These uridines are relocated during ribosome assembly from an open conformation to the internal core of the ribosome large subunit.

When pseudouridines cause stabilization of intermediate structures, locating the interfering positions can identify the 23S rRNA regions whose conformational changes are vital for progression of ribosome assembly. The interference sites are concentrated around the peptide exit tunnel and in the domain 0. The domain 0 consists of only 159 nt (35 uridines), 8 of which are interference sites. Such high sensitivity to rRNA modifications points to the structural reorganization of the domain 0 during large ribosome subunit assembly. Based on the conservation analysis of 23S rRNA-like molecules, Gerbi *et al*. suggested that the main function of the domain 0 is hidden in ribosome assembly. Our results support this proposal. The domain 0 of 23S rRNA is a part of the ancestral core of the LSU on the Bokov and Steinberg model (58). The domain 0 has a structural role in the 50S subunit, in addition to organizing other domains and forming part of the peptide exit tunnel, it holds A and P regions of ribosomal peptidyltransferase center in proximity (50). In addition, a U-turn motif in the 1130 region (interfering positions 1130 and 1132) is making several tertiary interactions with the domains 0 and V.

Accumulation of two types of subribosomal particles (42S and 48S) upon RluCD expression reflects inhibition of ribosome large subunit assembly progression at both early and late stages of assembly. Pseudouridylation pattern of 23S rRNA of both particles is similar. This suggests that conformational changes occur at the same 23S rRNA regions during early and late assembly events. Interactions between the 23S rRNA domains is expected to take place during early assembly. Formation of tertiary interactions on RNA inevitably needs rearrangements of RNA backbone around the interaction site. Therefore, it is not surprising to find pseudouridine interference sites around the regions involved in tertiary interaction. All interference sites but U2111 are in the vicinity of long-range tertiary interactions. Activation of the ribosomal PTC is a final step of ribosome large subunit biogenesis. Interference site U1944 is the neighbor of the A loop of ribosomal PTC. Therefore, pseudouridine at position 1944 can hinder activation of the PTC during ribosome assembly.

SUPPLEMENTARY DATA

Supplementary Data are available at NAR Online.

ACKNOWLEDGEMENTS

The authors thank M. O'Connor (University of Missoury-Kansas City) for help, D. Wilson (Munich), A. Ainelo and T. Tamm (University of Tartu) for critically reading the manuscript.

FUNDING

Institutional Research Funding projects of the Estonian Ministry of Education and Research [IUT20-21]. Funding for open access charge: Research Grant Award [IUT20-21].
Conflict of interest statement. None declared.

REFERENCES

1. Melnikov,S., Ben-Shem,A., Garreau de Loubresse,N., Jenner,L., Yusupova,G. and Yusupov,M. (2012) One core, two shells: bacterial and eukaryotic ribosomes. *Nat. Struct. Mol. Biol.*, **19**, 560–567.
2. Held,W.A., Ballou,B., Mizushima,S. and Nomura,M. (1974) Assembly mapping of 30 S ribosomal proteins from Escherichia coli. Further studies. *J. Biol. Chem.*, **249**, 3103–3111.

3. Herold,M. and Nierhaus,K.H. (1987) Incorporation of six additional proteins to complete the assembly map of the 50 S subunit from Escherichia coli ribosomes. *J. Biol. Chem.*, **262**, 8826–8833.
4. Talkington,M.W., Siuzdak,G. and Williamson,J.R. (2005) An assembly landscape for the 30S ribosomal subunit. *Nature*, **438**, 628–632.
5. Davis,J.H., Tan,Y.Z., Carragher,B., Potter,C.S., Lyumkis,D. and Williamson,J.R. (2016) Modular assembly of the bacterial large ribosomal subunit. *Cell*, **167**, 1610–1622.
6. Stern,S., Powers,T., Changchien,L.M. and Noller,H.F. (1989) RNA-protein interactions in 30S ribosomal subunits: folding and function of 16S rRNA. *Science*, **244**, 783–790.
7. Holmes,K.L. and Culver,G.M. (2004) Mapping structural differences between 30S ribosomal subunit assembly intermediates. *Nat. Sruct. Mol. Biol.*, **11**, 179–186.
8. Kim,H., Abeysirigunawarden,S.C., Chen,K., Mayerle,M., Ragunathan,K., Luthey-Schulten,Z., Ha,T. and Woodson,S.A. (2014) Protein-guided RNA dynamics during early ribosome assembly. *Nature*, **506**, 334–338.
9. Traub,P. and Nomura,M. (1969) Structure and function of Escherichia coli ribosomes. VI. Mechanism of assembly of 30 s ribosomes studied in vitro. *J. Mol. Biol.*, **40**, 391–413.
10. Franceschi,F.J. and Nierhaus,K.H. (1990) Ribosomal proteins L15 and L16 are mere late assembly proteins of the large ribosomal subunit. Analysis of an Escherichia coli mutant lacking L15. *J. Biol. Chem.*, **265**, 16676–16682.
11. Besancon,W. and Wagner,R. (1999) Characterization of transient RNA-RNA interactions important for the facilitated structure formation of bacterial ribosomal 16S RNA. *Nucleic Acids Res.*, **27**, 4353–4362.
12. Liiv,A. and Remme,J. (2004) Importance of transient structures during post-transcriptional refolding of the pre-23S rRNA and ribosomal large subunit assembly. *J. Mol. Biol.*, **342**, 725–741.
13. Yassin,A., Fredrick,K. and Mankin,A.S. (2005) Deleterious mutations in small subunit ribosomal RNA identify functional sites and potential targets for antibiotics. *Proc. Natl. Acad. Sci. U.S.A.*, **102**, 16620–16625.
14. Yassin,A. and Mankin,A.S. (2007) Potential new antibiotic sites in the ribosome revealed by deleterious mutations in RNA of the large ribosomal subunit. *J. Biol. Chem.*, **282**, 24329–24342.
15. Charollais,J., Pflieger,D., Vinh,J., Dreyfus,M. and Iost,I. (2003) The DEAD-box RNA helicase SrmB is involved in the assembly of 50S ribosomal subunits in Escherichia coli. *Mol. Microbiol.*, **48**, 1253–1265.
16. Charollais,J., Dreyfus,M. and Iost,I. (2004) CsdA, a cold-shock RNA helicase from Escherichia coli, is involved in the biogenesis of 50S ribosomal subunit. *Nucleic Acids Res.*, **32**, 2751–2759.
17. Peil,L., Virumae,K. and Remme,J. (2008) Ribosome assembly in Escherichia coli strains lacking the RNA helicase DeaD/CsdA or DbpA. *FEBS J.*, **275**, 3772–3782.
18. Siibak,T. and Remme,J. (2010) Subribosomal particle analysis reveals the stages of bacterial ribosome assembly at which rRNA nucleotides are modified. *RNA*, **16**, 2023–2032.
19. Xu,Z., O'Farrell,H.C., Rife,J.P. and Culver,G.M. (2008) A conserved rRNA methyltransferase regulates ribosome biogenesis. *Nat. Struct. Mol. Biol.*, **15**, 534–536.
20. Arai,T., Ishiguro,K., Kimura,S., Sakaguchi,Y., Suzuki,T. and Suzuki,T. (2015) Single methylation of 23S rRNA triggers late steps of 50S ribosomal subunit assembly. *Proc. Natl. Acad. Sci. U.S.A.*, **112**, E4707–E4716.
21. Ofengand,J. and Del Campo,M. (2004) *Modified Nucleotides of Escherichia Coli Ribosomal RNA*. ASM Press, Washington, DC.
22. Carlile,T.M., Rojas-Duran,M.F., Zinshteyn,B., Shin,H., Bartoli,K.M. and Gilbert,W.V. (2014) Pseudouridine profiling reveals regulated mRNA pseudouridylation in yeast and human cells. *Nature*, **515**, 143–146.
23. Lovejoy,A.F., Riordan,D.P. and Brown,P.O. (2014) Transcriptome-wide mapping of pseudouridines: pseudouridine synthases modify specific mRNAs in S. cerevisiae. *PLoS One*, **9**, e110799.
24. Schwartz,S., Bernstein,D.A., Mumbach,M.R., Jovanovic,M., Herbst,R.H., Leon-Ricardo,B.X., Engreitz,J.M., Guttman,M., Satija,R., Lander,E.S. *et al.* (2014) Transcriptome-wide mapping reveals widespread dynamic-regulated pseudouridylation of ncRNA and mRNA. *Cell*, **159**, 148–162.
25. Ofengand,J. (2002) Ribosomal RNA pseudouridines and pseudouridine synthases. *FEBS Lett.*, **514**, 17–25.
26. Ofengand,J., Malhotra,A., Remme,J., Gutgsell,N.S., Del Campo,M., Jean-Charles,S., Peil,L. and Kaya,Y. (2001) Pseudouridines and pseudouridine synthases of the ribosome. *Cold Spring Harb. Symp. Quant. Biol.*, **66**, 147–159.
27. Gutgsell,N.S., Deutscher,M.P. and Ofengand,J. (2005) The pseudouridine synthase RluD is required for normal ribosome assembly and function in Escherichia coli. *RNA*, **11**, 1141–1152.
28. Ejby,M., Sorensen,M.A. and Pedersen,S. (2007) Pseudouridylation of helix 69 of 23S rRNA is necessary for an effective translation termination. *Proc. Natl. Acad. Sci. U.S.A.*, **104**, 19410–19415.
29. O'Connor,M. and Gregory,S.T. (2011) Inactivation of the RluD pseudouridine synthase has minimal effects on growth and ribosome function in wild-type Escherichia coli and Salmonella enterica. *J. Bacteriol.*, **193**, 154–162.
30. Dreyfus,M. and Heurgue-Hamard,V. (2011) Termination troubles in Escherichia coli K12. *Mol. Microbiol.*, **79**, 288–291.
31. Conrad,J., Sun,D., Englund,N. and Ofengand,J. (1998) The rluC gene of Escherichia coli codes for a pseudouridine synthase that is solely responsible for synthesis of pseudouridine at positions 955, 2504, and 2580 in 23 S ribosomal RNA. *J. Biol. Chem.*, **273**, 18562–18566.
32. Vaidyanathan,P.P., Deutscher,M.P. and Malhotra,A. (2007) RluD, a highly conserved pseudouridine synthase, modifies 50S subunits more specifically and efficiently than free 23S rRNA. *RNA*, **13**, 1868–1876.
33. Mizutani,K., Machida,Y., Unzai,S., Park,S.Y. and Tame,J.R. (2004) Crystal structures of the catalytic domains of pseudouridine synthases RluC and RluD from Escherichia coli. *Biochemistry*, **43**, 4454–4463.
34. Leppik,M., Peil,L., Kipper,K., Liiv,A. and Remme,J. (2007) Substrate specificity of the pseudouridine synthase RluD in Escherichia coli. *FEBS J.*, **274**, 5759–5766.
35. Datsenko,K.A. and Wanner,B.L. (2000) One-step inactivation of chromosomal genes in Escherichia coli K-12 using PCR products. *Proc. Natl. Acad. Sci. U.S.A.*, **97**, 6640–6645.
36. Baba,T., Ara,T., Hasegawa,M., Takai,Y., Okumura,Y., Baba,M., Datsenko,K.A., Tomita,M., Wanner,B.L. and Mori,H. (2006) Construction of Escherichia coli K-12 in-frame, single-gene knockout mutants: the Keio collection. *Mol. Syst. Biol.*, **2**, doi:10.1038/msb4100050.
37. Ofengand,J. and Bakin,A. (1997) Mapping to nucleotide resolution of pseudouridine residues in large subunit ribosomal RNAs from representative eukaryotes, prokaryotes, archaebacteria, mitochondria and chloroplasts. *J. Mol. Biol.*, **266**, 246–268.
38. Liiv,A., Karitkina,D., Maivali,U. and Remme,J. (2005) Analysis of the function of E. coli 23S rRNA helix-loop 69 by mutagenesis. *BMC Mol. Biol.*, **6**, 18.
39. Gehrke,C.W. and Kuo,K.C. (1989) Ribonucleoside analysis by reversed-phase high-performance liquid chromatography. *J. Chromatogr.*, **471**, 3–36.
40. Ofengand,J., Del Campo,M. and Kaya,Y. (2001) Mapping pseudouridines in RNA molecules. *Methods*, **25**, 365–373.
41. Gutgsell,N.S., Del Campo,M., Raychaudhuri,S. and Ofengand,J. (2001) A second function for pseudouridine synthases: a point mutant of RluD unable to form pseudouridines 1911, 1915, and 1917 in Escherichia coli 23S ribosomal RNA restores normal growth to an RluD-minus strain. *RNA*, **7**, 990–998.
42. Yusupov,M.M., Yusupova,G.Z., Baucom,A., Lieberman,K., Earnest,T.N., Cate,J.H. and Noller,H.F. (2001) Crystal structure of the ribosome at 5.5 A resolution. *Science*, **292**, 883–896.
43. Clatterbuck Soper,S.F., Dator,R.P., Limbach,P.A. and Woodson,S.A. (2013) In vivo X-ray footprinting of Pre-30S ribosomes reveals chaperone-dependent remodeling of late assembly intermediates. *Mol. Cell*, **52**, 506–516.
44. Russell,S.P. and Limbach,P.A. (2013) Evaluating the reproducibility of quantifying modified nucleosides from ribonucleic acids by LC-UV-MS. *J. Chromatogr. B Analyt. Technol. Biomed. Life Sci.*, **923–924**, 74–82.
45. Bugl,H., Fauman,E.B., Staker,B.L., Zheng,F., Kushner,S.R., Saper,M.A., Bardwell,J.C. and Jakob,U. (2000) RNA methylation under heat shock control. *Mol. Cell*, **6**, 349–360.

46. Caldas,T., Binet,E., Bouloc,P., Costa,A., Desgres,J. and Richarme,G. (2000) The FtsJ/RrmJ heat shock protein of Escherichia coli is a 23 S ribosomal RNA methyltransferase. *J. Biol. Chem.*, **275**, 16414–16419.
47. Srivastava,A.K. and Schlessinger,D. (1988) Coregulation of processing and translation: mature 5' termini of Escherichia coli 23S ribosomal RNA form in polysomes. *Proc. Natl. Acad. Sci. U.S.A.*, **85**, 7144–7148.
48. King,T.C., Sirdeshmukh,R. and Schlessinger,D. (1984) RNase III cleavage is obligate for maturation but not for function of Escherichia coli pre-23S rRNA. *Proc. Natl. Acad. Sci. U.S.A.*, **81**, 185–188.
49. Lindahl,L. (1975) Intermediates and time kinetics of the in vivo assembly of Escherichia coli ribosomes. *J. Mol. Biol.*, **92**, 15–37.
50. Petrov,A.S., Bernier,C.R., Hershkovits,E., Xue,Y., Waterbury,C.C., Hsiao,C., Stepanov,V.G., Gaucher,E.A., Grover,M.A., Harvey,S.C. *et al.* (2013) Secondary structure and domain architecture of the 23S and 5S rRNAs. *Nucleic Acids Res.*, **41**, 7522–7535.
51. Dunin-Horkawicz,S., Czerwoniec,A., Gajda,M.J., Feder,M., Grosjean,H. and Bujnicki,J.M. (2006) MODOMICS: a database of RNA modification pathways. *Nucleic Acids Res.*, **34**, D145–D149.
52. Chow,C.S., Lamichhane,T.N. and Mahto,S.K. (2007) Expanding the nucleotide repertoire of the ribosome with post-transcriptional modifications. *ACS Chem. Biol.*, **2**, 610–619.
53. Hudson,G.A., Bloomingdale,R.J. and Znosko,B.M. (2013) Thermodynamic contribution and nearest-neighbor parameters of pseudouridine-adenosine base pairs in oligoribonucleotides. *RNA*, **19**, 1474–1482.
54. Kierzek,E., Malgowska,M., Lisowiec,J., Turner,D.H., Gdaniec,Z. and Kierzek,R. (2014) The contribution of pseudouridine to stabilities and structure of RNAs. *Nucleic Acids Res.*, **42**, 3492–3501.
55. Jiang,J., Aduri,R., Chow,C.S. and SantaLucia,J. Jr (2014) Structure modulation of helix 69 from Escherichia coli 23S ribosomal RNA by pseudouridylations. *Nucleic Acids Res.*, **42**, 3971–3981.
56. Noeske,J., Wasserman,M.R., Terry,D.S., Altman,R.B., Blanchard,S.C. and Cate,J.H. (2015) High-resolution structure of the Escherichia coli ribosome. *Nat. Struct. Mol. Biol.*, **22**, 336–341.
57. Mulder,A.M., Yoshioka,C., Beck,A.H., Bunner,A.E., Milligan,R.A., Potter,C.S., Carragher,B. and Williamson,J.R. (2010) Visualizing ribosome biogenesis: parallel assembly pathways for the 30S subunit. *Science*, **330**, 673–677.
58. Bokov,K. and Steinberg,S.V. (2009) A hierarchical model for evolution of 23S ribosomal RNA. *Nature*, **457**, 977–980.